Wireless Capacitive Based ECG Sensing for Feature Extraction and Mobile Health Monitoring

Johan Wannenburg, Reza Malekian*, *Senior Member, IEEE*, *and GerhardP.Hancke*, *Fellow, IEEE*

***Abstract*—In this research the concept of a wireless wearable device capable of measuring ECG and respiration rate through the use of non-contact capacitive based electrodes was designed and implemented. Both ECG and respiration rate (RR) were measured using only the active electrodes and an analog conditioning circuit. The device utilises BLE for low powered wireless communication to the remote server. The measured data is used to calculate HRV, RR and extract ECG related features. It was found that the use of non-contact active chest electrodes are a viable approach for measurement. The system focuses on user comfort and the minimisation the ratio of the number of wearable sensors to sensed physiological parameters.**

***Keywords*—ECG, respiration rate, capacitive sensing, active electrode, wireless wearable sensing, remote health monitoring.**

I. Introduction

THE continuous development and improvement of current technology creates a platform where health monitoring has the potential to become pervasive and ubiquitous. Current developments in mobile health monitoring are paving the way for the fulfilment of the "Pervasive Healthcare" vision, this vision seeks to provide anyone with healthcare, anytime, anywhere. It also seeks to improve coverage while maintaining a fair standard of quality [1]. Continuous mobile health monitoring is a promising prospect, since it adheres to this vision. The focus of continuous health monitoring would be to accurately measure the physiological parameters of a user in an unobtrusive manner, therefore, not interfering with the user's everyday activity. Some of these parameters include heart rate, skin temperature, blood pressure, respiration rate and saturation of blood oxygen [2], [3]. These parameters could provide medical care stations with the relevant information to distinguish between normal activity and a medical emergency. Mobile health monitoring also provides the possibility of contributing to medical research, where certain medical conditions can be associated with specific observations of the physiological parameters.

New innovative ways of acquiring the above-mentioned parameters are constantly being developed and explored. This work focuses on current techniques relating to the extraction of heart rate activity, electrocardiogram (ECG) and respiration rate. The physiological parameters are acquired through the use of capacitive based non-contact active electrodes, the electrodes are placed on the user's chest, over a worn vest. Signals are captured and conditioned by an analog frontend where ECG and respiration rate (RR) is separated by utilizing a differential separation filter. The system makes use of Bluetooth v4.0 or Bluetooth low energy (BLE) for wireless communication between the wearable device and remote server.

The techniques explored in this system seek to contribute to the development of a device that adheres to the vision of pervasive healthcare. Thus the system explores approaches that are unobtrusive and minimise discomfort to the user; they also allow the user to continue with his/her everyday activities, while maintaining high accuracy. The research is also driven to reduce the number of sensors connected to a patient for health monitoring. By measuring both ECG and RR with the active electrode configuration, two physiological parameters are measured with a single sensing device. A reduction in the number of connected sensors has the potential to improve user comfort, as well as, decrease system complexity [4], [5] . The measured vitals can also be monitored remotely, therefore, in the case of a medical emergency services could be dispatched to assist the user in distress. The design also focuses on employing a low powered technique for wireless communication, thus the use of BLE was investigated.

This paper is structured as follows: Section II gives an explanation on the required background information on ECG and respiration rate. Section III gives a brief overview of the system and its functions. The implemented design is explained thoroughly in section IV including key circuit designs. The results are shown and discussed in detail in section V. Any future work or improvements are discussed in section VI and finally, the paper is concluded in section VII.

II. Background Relating to ECG and Respiration Rate

A. The Electrocardiogram

The electrocardiogram (ECG) is one of the most widely used techniques in health monitoring, it provides valuable information about the cardiovascular system by means of evaluating electrical heart activity [6], [7]. ECG can be used to detect any cardiovascular disease or related abnormalities in heart functionality [8]. This principle can be implemented in continuous health monitoring by taking periodic measurements of a patient's vitals. The ECG signal can also be used to determine heart rate variability (HRV), as well as, for the detection of anomalies in heart activity, such as arrhythmia and tachycardia [6].

The ECG signal waveform is a periodic signal that is usually made up of 6 distinct parts, PQRSTU (U appears very rarely)

Johan Wannenburg is with the Department of Electrical, Electronic and Computer Engineering, University of Pretoria, Pretoria, 0002, South Africa.

Reza Malekian is Head of the Advanced Sensor Networks Research Group at the Department of Electrical, Electronic and Computer Engineering, University of Pretoria, Pretoria, 0002, South Africa. (email: reza.malekian@ieee.org)

Gerhard P. Hancke is with the Department of Electrical, Electronic and Computer Engineering, University of Pretoria, Pretoria, 0002, South Africa.

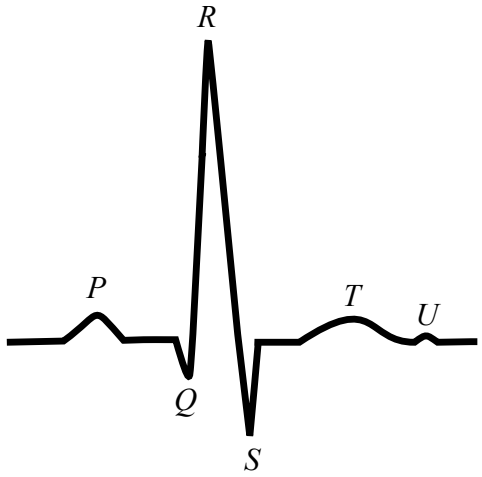

Fig. 1. Features of the normal ECG signal.

these can be observed in figure 1. Of these 6 key components, the QRS is regarded as the most important since this can give a clear indication of any cardiac related problems [9]. The QRS complex shows when ventricular depolarisation takes place, resulting in a contraction of the ventricles [10]. The R peak is also crucial, since the interval between successive R peaks, known as the R-R interval can be used to extract a patient's heart rate or HRV [11]. These parameters have a very specific relation with regard to each other, in both their succession in time and amplitude; and are thus useful in deducing when a cardiac emergency occurs.

The measured ECG signal is minute and usually has an amplitude of approximately 0.1-1 mV [12]. Therefore, the acquisition method is very important and determines the quality of the sampled signal. According to Webster the most important frequency components that make up the ECG signal lie between 0.01-250 Hz. Therefore, this frequency range should be isolated for evaluation and feature extraction [13]. The frequency range to be isolated depends greatly on which vitals or features will be derived from the signal, for instance deriving HRV requires evaluation of frequencies between 0.5 and 3.67 Hz which translates to 30-220 beats per minute (BPM) [2].

1) Common ECG Artifacts: A measured ECG signal may be contaminated with various noise sources, known as artifacts; and they could potentially corrupt the signal or result in false alarms [10]. Therefore, it is crucial that these effects are minimised and even eradicated where possible. There are 4 main artifacts that have been identified when measuring ECG. They are known as baseline wandering, AC interference, muscle tremor and motion artifacts. Figure 2 shows a visual representation of the common artifacts.

Baseline wandering is an artifact where the signal's baseline slowly wanders, and is caused by electrode movement. The electrode movement could be related to body movement or breathing activity [10], [14]. AC interference is an artifact that causes the signal amplitude to vary, this is due to electrical power leakage, poor grounding techniques or being in a proximity that is too close to other electrical equipment [10]. When irregular narrow and rapid spikes occur in the ECG signal could be as a result of muscle tremors. Possible causes could be shivering, EMG signals or Parkinson's disease [10]. Motion artifacts are the most common of the ECG signal interferences, and usually results in a large irregular swing in the baseline affecting the amplitude drastically. This artifact could be caused by epidermal signals, coughing or ambulation [8], [10].

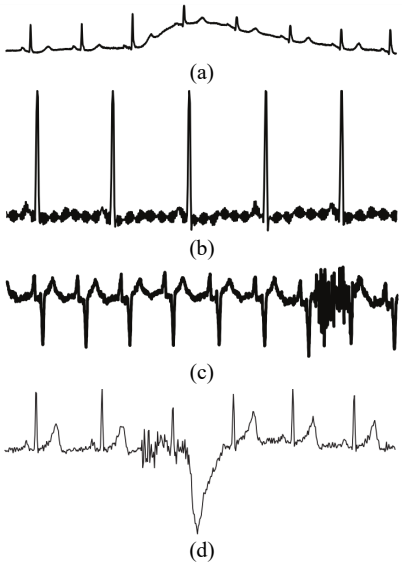

Fig. 2. A Summary of the common artifacts in ECG signals. (a) Baseline wander, (b) AC interference, (c) Muscle tremor and (d) Motion artifact.

B. ECG Acquisition Techniques

ECG signals can be measured by various combinations of surface or implanted electrodes that measure a differential voltage. The measured voltage is due to an electromagnetic signal caused by the activity of the cardiac muscles [9]. Electrodes can be contact electrodes, where the electrodes are placed directly on the skin and make use of resistive coupling. They could also be non-contact, which means that there is no direct contact with the patient's skin and sensing takes place through capacitive coupling [9]. The total number of electrodes is another important aspect since when they are appropriately placed the measured waveforms can provide useful information regarding specific electrical activity throughout the heart.

Usually non-invasive electrodes are implemented when measuring ECG potentials. The conventional clinical method of acquiring ECG employs the use of wet electrodes or Ag/AgCl electrodes, these are electrodes that are placed directly on the skin [12]. They are generally placed on specific areas on the patient's body (arms, hands, legs and chest) and require that the placed area be cleaned and covered with a specific gel to increase the conductivity. These electrodes are usually only made of a metallic contact area and are therefore passive, they provide very accurate signal, but are not ideal for continuous monitoring. They cause skin irritation and allergic reactions when kept on the skin for long periods of time [7].

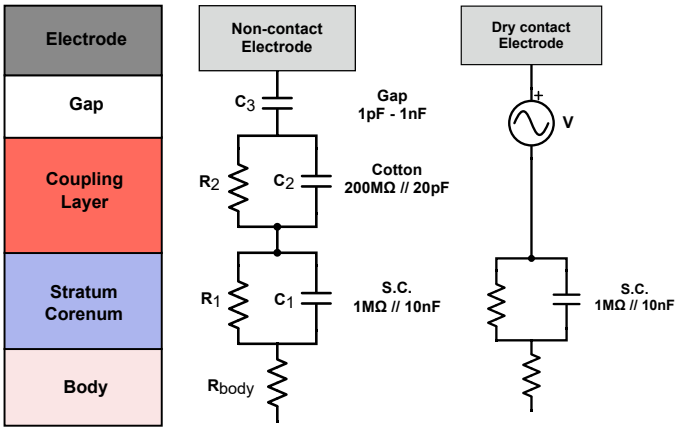

Fig. 3. Skin and electrode interface model.

When deciding on an electrode interface for continuous measurement focus should be placed on a method that is ideal for prolonged use and one that provides maximum convenience for the user. Therefore, dry and non-contact electrodes could be possible candidates for continuous ECG measurement. Dry-contact electrodes are when a metal surface is placed directly on the patient's skin without a conductive gel, this method still requires direct skin contact and could thus result in skin irritation [7]. To solve this problem a non-contact electrode model is implemented, here a thin layer of insulating material separates the skin and the metal electrode surface. This method has successfully been used in research to measure ECG signals [7], [8], [12], [15]. According to Y. Chi et al. their research shows that non-contact electrodes if buffered and shielded, can perform as well as if not better than wet electrodes [12]. The non-contact electrode method is capable of long term measurement without disturbing the user.

1) Capacitively Coupled Sensing: Figure 3 explains the interface between the human skin and two electrode configurations. When measuring potentials on the skin an impedance is generated by the body and the Stratum Corenum. This impedance consists of a parallel combination of resistive and capacitive components. When the electrode makes direct contact with the skin, such as in the case of the wet/dry electrode, the measured signal follows the resistive path. This is due to the fact that the impedance caused by the resistive component is lower than that of the capacitive component. When the non-contact electrode method is implemented the signal follows the other path, hence resulting in capacitive coupling [7], [12]. In the non-contact model a coupling layer is usually added, namely, the thin insulator. This insulator can either be a thin film on the electrode or a fabric such as wool or cotton, meaning that it can be measured on top of a layer of clothing [6]. The one disadvantage of capacitive based electrodes is the fact that they are very susceptible to noise when it comes to motion artifacts or body movement [16].

2) Active vs. Passive Elecrodes: Non-contact electrodes usually suffer when it comes to signal quality since the capacitive components produce a higher impedance than that of the direct contact electrodes. As mentioned passive electrodes are when only a measuring surface area is placed on the skin and transferred to the processing node via electrical cabling. This could cause increased signal noise in the continuous measurement approach since the cabling may be exposed to electromagnetic interference (EMI), depending on the user's environment. When impedance across a cable is exposed to EMI a current is induced, and according to Ohm's law the product of the induced current and impedance result in a voltage. In this case the induced current is as a result of 50/60 Hz AC signals [2], thus the voltage generated is not necessarily only the measured signal, but mostly noise. Therefore, higher impedances will result in much higher noise levels. Active electrodes seek to solve this problem since they provide on-electrode pre-processing. In an active electrode the high input impedance is converted to a much lower output impedance through the use of an active buffer stage, resulting in lower noise levels [17].

C. Respiration Rate

Respiration rate (RR) is one of the foremost external signs that can give vital information on whether or not a person is healthy [18]. Usually respiration tends to stay constant for all ages, except in the elderly. Under normal resting conditions RR is between 12 40 breaths per minute, which relates to a frequency range of between 0.2 0.67 Hz (usually below 1 Hz) [19]. RR is a crucial physiological parameter and can easily be measured in continuous health monitoring. Various methods exist in research and have been proven to be successful.

The implementation of plethysmography through inductive sensing is a popular method, and involves a strap worn around the chest or waist area [11], [19]. The strap is lined with a mesh of conducting wires, and the movement of the chest causes excitation which can be measured. Other methods that rely on ECG electrodes rather than a dedicated sensor also exist, for example the use of ECG derived respiration (EDR) [4] and Ballistocardiography [20]. EDR can be extracted from ECG since the signal is respiratory induced, due to external mechanisms. These include the change in impedance due to the change in lung volume [21], or a change in the heart vector as a result of displacement and orientation induced changes of the heart with respect to the electrodes [4].

Respiration rate is a vital physiological parameter that is vastly used in the study of apnea, more specifically sleep apnea [4], [22], [23]. The above-mentioned approaches are used in the monitoring and study of sleep apnea, however, a different approach was taken by X. Zhu et al. in their research. They make use of a pillow lined with pressure sensors, these sensors are then responsible to non-invasively measure the RR [23]. Thus RR is measured to study sleep apnea and its effects, and it can also be used in everyday continuous monitoring to determine whether a person's respiration rate is normal, abnormally slow (bradypnea) or abnormally fast (tachypnea); which could be an indication of the occurrence of a medical related event.

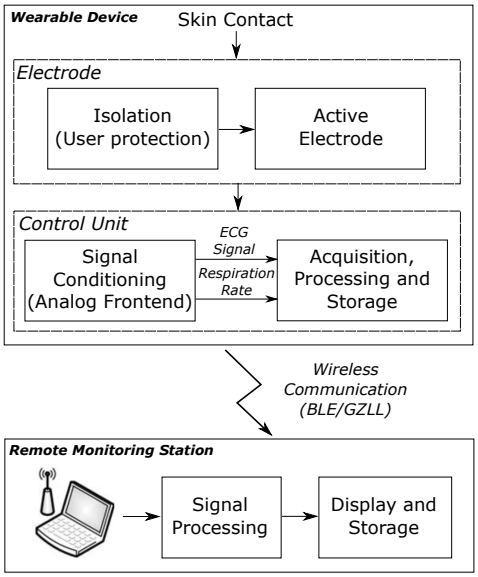

Fig. 4. Block diagram of designed system.

III. System Overview

The proposed system is made up of two main subsystems, the wearable device and the remote monitoring station. The wearable device is responsible for acquiring the ECG and RR signals, this subsystem consists of the active electrodes and the control unit. The active electrodes are placed on the user's chest with a strap, these electrodes are active in design in order to overcome the challenges described in section II above. The electrodes are placed on top of a cotton vest and measure a capacitively coupled signal. The electrodes offer isolation and a high input impedance in order to protect the user. The measured signals are passed to the control unit via shielded cabling and go through a conditioning process, this process will be explained in detail in section IV. The analog frontend is responsible for signal conditioning, such as filtering and amplification; as well as signal separation. The separated signals are then sampled by the ADC of a microcontroller and stored in a temporary buffer. The sampled signals are then sent to the remote monitoring station for processing and feature extraction.

The wearable device is battery powered and utilizes BLE, or the GZLL protocol for wireless communication with the server side. The remote monitoring station is implemented on a desktop computer and receives the data via a serial connection. The received signals are then evaluated and important features such as HRV, QRS complex and RR are extracted and evaluated. The evaluation of these features can then be used to detect when a medical emergency is being experienced, and notify a medical service. The main focus of this research is the design of the wearable device, the remote server was utilised to verify that the system works as intended, but could be further developed in future work. Figure 4 shows a visual depiction of the overall system flow.

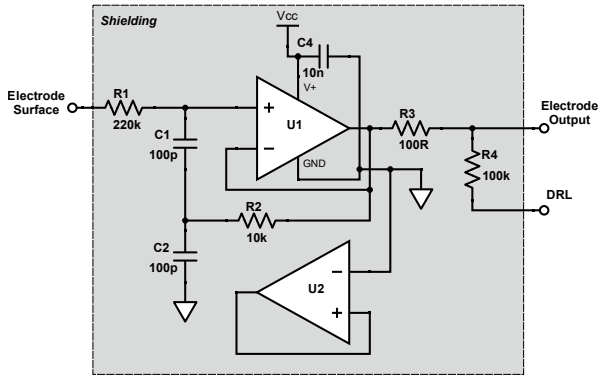

Fig. 5. Active electrode circuit diagram.

IV. Design Implementation

A. Active Electrode Design

As discussed active electrodes have a much higher input impedance than that of passive electrodes. This is crucial in protecting the user from any current injections through isolation. The design shown in figure 5 was used for the implementation of the two active electrodes used in this research. The design implements a buffer or voltage follower on the electrode that ensures that a high input impedance is maintained, as well as, a low output impedance. The op amp used for the buffer was a TLC272 LinCMOS device, this device has a very low input offset voltage (500 μV) and very low noise. These important factors are beneficial when measuring small scale signals such as ECG.

The electrode surface is coupled with the buffer through resistor R1, which is a large resistor for purposes of high input impedance. Components C1, C2 and R2 are used for protection and isolation of the user should there be any skin contact. Resistor R3 was selected as 100 Ω to serve as a low output impedance and to enforce impedance matching between the two electrodes. Component U2, a voltage follower was used to ensure a constant voltage supply and that the analog ground remains stable. Capacitor C4 was also used to ensure stability and used as a decoupling capacitor. The resistor R4 ensure a high input impedance to the right leg driver electrode (DRL) or the reference electrode. The entire circuit of the active electrode was shielded by placing it between 2 single layer PCBs, the output signal was also connected to the shielding

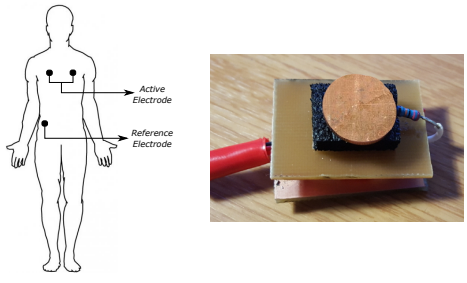

(a) *(b)*

Fig. 6. (a) The electrode placement and (b) the designed active electrode.

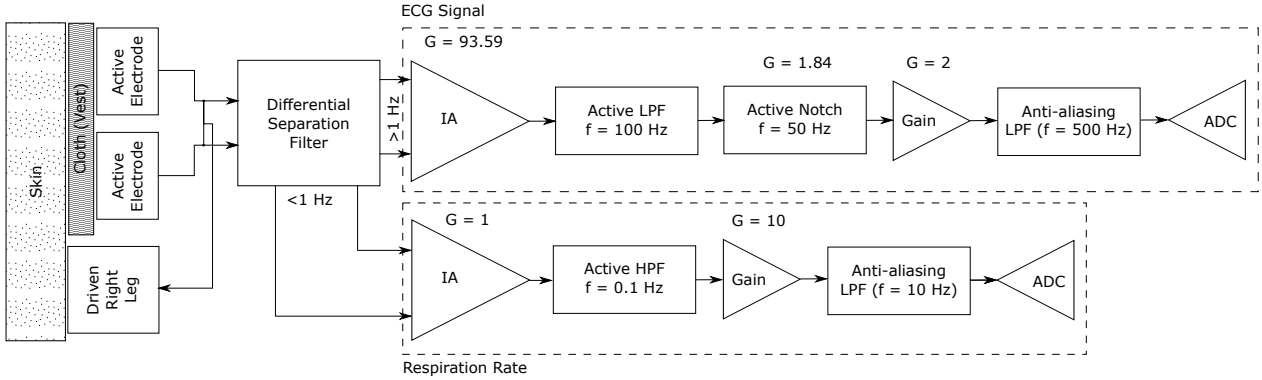

Fig. 7. Block diagram of the analog frontend.

to minimise signal noise.

An image of the actual electrode can be seen in figure 6. The electrode surface area is a round metal (copper) area with a diameter of approximately 17 mm which results in a surface area of roughly 107 mm^2. The resistor R1 can be seen connecting the electrode area with the buffer circuit. The explained shielding can also be seen here insulating the buffer circuit and shielding it from any AC interference. The active electrodes are placed on the chest area, while the reference (passive) electrode is placed on the left-hand side hip.

B. Analog Frontend

The analog frontend is the focal area of this design and is crucial in the sense that it is responsible for all signal conditioning and it ensures that the final signal output is of good quality. The active electrodes are placed on the subject's chest on a vest, while the reference electrode is placed directly on the skin. The reference electrode relays a common input signal back to the user's skin, which in this scenario is the systems ground. After the signal has been acquired by the electrodes it is passed to a separation differential filter, this block is responsible for separating the differential signal into two key signal components, (1) signals with a frequency above 1 Hz and the other (2) signals with frequencies below 1 Hz. This stage is essential for separating ECG and RR signal components. A full flow of the conditioning can be seen in figure 7.

1) ECG Conditioning: The first step in extracting the ECG signal is to pass the differential signal through an instrumentation amplifier (IA). The IA is responsible for rejecting all common mode signals between the two electrodes. The common mode signals induced here will be as a result of noise, which could be due to contact or the AC interference. An IA with a high common mode rejection ratio (CMRR) should be selected in order to minimise and suppress the effects of common mode noise. The IA selected in this design was the INA121 which is a FET-input low power device with a CMRR of 106 dB. The IA was also configured to amplify the minute ECG signal, it is beneficial to apply majority of the system's gain here since the higher the gain of the IA the better the CMRR. A gain of 93.59 V/V was selected through the relationship of R_G and G

$$G = 1 + \frac{50k\Omega}{R_G} \tag{1}$$

The gain was chosen as 100 V/V which resulted in

$$\begin{aligned} R_G &= 505.05 \\ &\approx 540\Omega \end{aligned} \tag{2}$$

R_G needs to be a standard value and was thus selected as 540 Ω and resulted in a gain of 93.59 V/V.

The signal was then passed through an active low pass filter with a cut off of 100 Hz. A 2nd order active filter was selected in order to get an appropriate roll off or steep cut off, since the frequency range of interest is quiet small. A Sallen-Key KRC filter was used in this design and a frequency of 100 Hz was selected since this would retain enough information in the ECG signal for feature extraction and analysis.

The notch filter is essential since it is required to remove AC interference left in the circuit. The stopband frequency was selected as 50 Hz which is the frequency of powerline AC voltages in the area. The active twin T notch topology was used in this design since it generally provides adequate noise suppression. This stage also provided some amplification to the signal for purposes of stability, this gain was calculated as 1.84 V/V. The bandwidth of the notch filter was measured as 65 Hz.

A non-inverting gain stage was implemented to amplify the signal to the full-scale range of the microcontroller's ADC. This concept is used to improve the quality of the sampled signal when lower resolution ADCs are utilised, such as in this case where the resolution is 10 bits. The microcontroller is a Cortex M0 processor and is a 3.3 V device, thus the ADC range would be between 03.3 V. It was determined that the signal only by amplified with a gain of 2 V/V in order to obtain a full-scale signal swing.

The final stage before being sampled was to implement a low pass anti-aliasing filter to band limit the ECG signal. This stage utilised a passive filter design to save resources and keep the size to a minimum. Based on the system design all ECG signal components below 100 Hz are to be sampled, this means that according to the Nyquist criterion the sampling

rate should be at least double, thus resulting in 200 Hz. The anti-aliasing filter allows for oversampling which creates a wider separation between the desired signal and noise components. In this design a sampling rate of 500 Hz was selected to effectively oversample the signal. The overall gain of the ECG conditioning circuit was found to be 344.41 V/V.

2) Respiration Rate Conditioning: Respiration rate is usually detected from very low frequency signals, typically below 1 Hz, which results in a very small bandwidth. Therefore, it is important that active filters are used to ensure steep cut offs for optimal results. After the low frequency components have been extracted from the differential separation filter the signal is passed through an IA to remove common mode noise. The signal is then passed through an active high pass filter with a cut off frequency of 0.1 Hz. Once again a Sallen-Key 2nd order topology was utilised for increased performance.

This filter is used to remove DC components and result in a signal oscillating about the reference voltage. The entire system is driven from a single source power supply which means that a reference other than ground should be selected, which is the default case in dual supply systems. The reference, or virtual ground was selected as half of the supply voltage (3.3 V), which resulted in a reference of 1.65 V. Half of the supply voltage is deemed optimal, should the signal be amplified to full scale no clipping will take place.

After the filtering, the signal was amplified by means of a non-inverting amplifier stage. The signal was amplified by a gain of 10 V/V and passed through an anti-aliasing filter with a cut off frequency of 10 Hz. This was selected so that the signal can be oversampled to maintain quality.

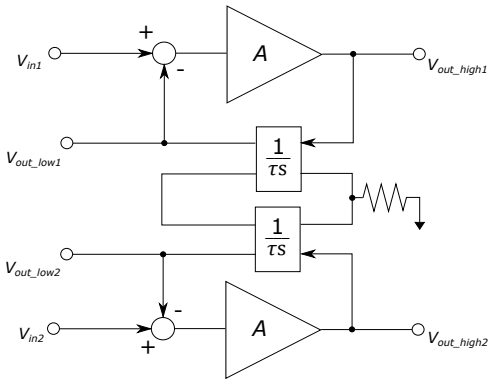

Fig. 8. Differential separation filter block diagram.

C. Differential Separation Filter

The susceptibility to motion artifacts of the capacitively coupled electrodes could be seen as a disadvantage when trying to measure ECG signals. However, this increased sensitivity could be used as an advantage when measuring respiration rate from the slow varying frequency caused by movement of the ECG electrodes on the chest [16]. This low frequency can be separated from the high frequency ECG signal components through the implementation of a separation filter. To implement a separation filter for a differential signal while maintaining a high CMRR, a mirroring technique is applied to the single-ended separation filter design [24].

Referring to figure 8 it is observed that there are two inputs V_{in1} and V_{in2}, and 2 sets of outputs; one for frequencies above 1 Hz (high) and one for frequencies below 1 Hz (low). Considering the relationship between V_{out_high} and V_{in} it is seen that V_{out_high} is integrated with a time constant τ and fed back to the input negatively [16]. Since this difference is amplified with a factor A, a transfer function for $G_{high}(s)$ is given by

$$G_{high}(s) = \frac{V_{out\_high}}{V_{in}} = \frac{\tau s}{1 + \frac{\tau s}{A}} \tag{3}$$

The equation in (3) represents the transfer function of a 1st order high pass Butterworth filter. V_{out_low} is produced by the integration of V_{out_high} which results in a transfer function $G_{low}(s)$

$$G_{low}(s) = G_{high}(s) \cdot \frac{1}{\tau s} = \frac{1}{1 + \frac{\tau s}{A}} \tag{4}$$

Equation (4) shows the relationship between V_{out_low} and V_{in}, and results in a transfer function representing that of a 1st order low pass Butterworth filter. If this concept is applied and τ is configured so that the cut off frequency is 1 Hz the circuit will function as proposed.

The separation filter consists of two sets of subtractors, amplifiers and integrators [16]. Figure 9 shows the circuit diagram of a single side of the implemented differential separation filter, therefore, the implemented circuit consists of a mirrored version as well. The subtractor output voltage with a unity gain had the following relationship with the resistor values:

$$V_{out} = (V_2 - V_1)\left(\frac{R_2}{R_1}\right) \tag{5}$$

Where resistors R1-R4 where selected as 1 $k\Omega$ for a gain of 1 V/V, and V_2 = V_{in} and V_1 = V_{out_low}. The amplifier was implemented as a voltage follower with a unity gain, since amplification will be done by the IA. The integrator was implemented using an active non-inverting integrator topology. The integrator has the transfer function $H(s)$

$$H(s) = \frac{1}{\tau s} \tag{6}$$

Where τ is determined by components R and C, thus in figure 9 R6-R9 and C1. τ is selected as 0.16 sec (R = 160 $k\Omega$ and C = 1 μF) to give a cut off frequency of 1 Hz.

D. DC Removal in ECG Conditioning

Once the ECG signal has passed through the IA it will have undergone amplification, the problem with this amplification is that it will also amplify any existing DC components as well. There is a possibility that DC components might still exist based on the fact that the differential separation filter is only the equivalent of a 1st order filter. In order to remove any accumulated DC offset an integrator is implemented at the

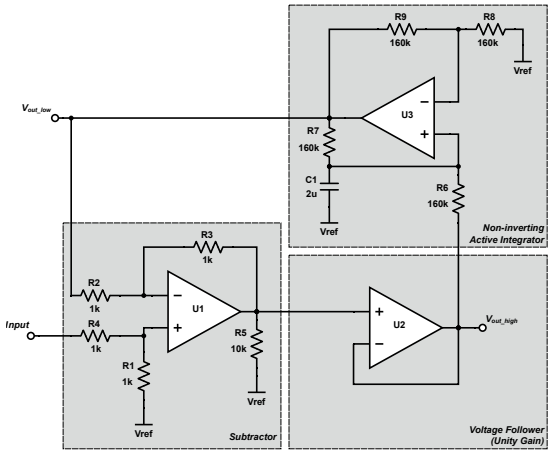

Fig. 9. Differential separation filter circuit diagram.

output of the IA. The integrator input is the output of the IA while the output is fed back to the reference voltage pin of the IA. The integrator was designed to have a cut off frequency of 0.5 Hz resulting in the components and configuration in figure 10.

E. Driven Right Leg (DRL) and Reference Electrode

The driven right leg (DRL) is a technique used to employ common mode biasing and active grounding [9]. This technique is useful for common mode noise reduction and works by taking the average voltages of the two input terminals. The average voltage is amplified, inverted and then fed back to the reference or user's skin. The significance of the circuit is that it does not remove any differential signal components, it only suppresses common mode noise.

In this design the average voltage is first passed through a buffer stage to produce a high input impedance for user protection, thereafter it is inverted, amplified and passed to the reference electrode. The reference electrode implemented consists only of a small metal contact area connected to a shielded cable for noise suppression.

F. BLE/GZLL Wireless Communication

As mentioned in the system overview, the wireless communication technique utilised in this design was based on

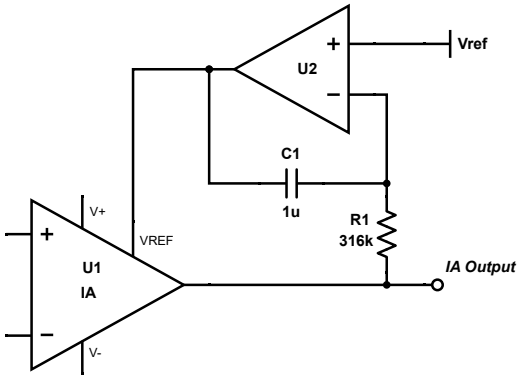

Fig. 10. DC removal design circuit.

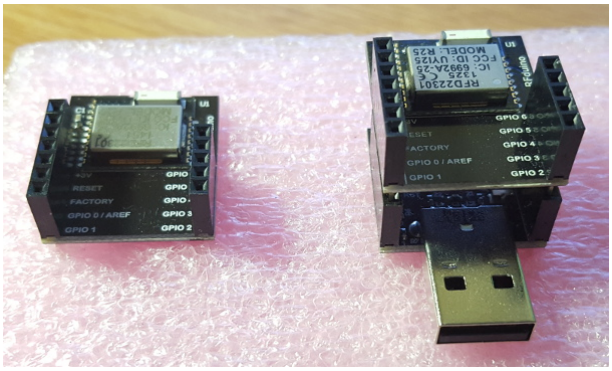

Fig. 11. The 2 BLE nodes used for processing and wireless communication.

Bluetooth v4.0 or BLE. The processing node used in the control unit is based on the nRF51822 Bluetooth chip from Nordic Semiconductor. It's built on an ARM Cortex M0 32-bit processor architecture with BLE capabilities. Two of these nodes will be used in the system, one on the wearable device for data acquisition, processing and transmission/reception and the other on the server side for reception/transmission. Figure 11 shows the two nodes, where one has a USB interface to communicate with the remote server via serial port.

The protocol used between the two devices is GZLL or gazell which is built on BLE, it is designed to create a robust wireless link between a host and up to 8 devices in a star network topology. The protocol is low powered and takes advantage of the fact that the host or remote side is always powered, while the device only transmits when necessary. GZLL is capable of a 2 Mbps communication link and uses 12 mA for transmission. The protocol makes use of a packet that can carry a payload of up to 32 bytes.

The wearable device is set up in such a manner that it acquires ECG and RR samples and stores them until the transmission buffer is full before it transmits. This approach means that data is not continuously sent but rather in bursts which results in more efficient use of power. Based on the sampling rates the device sends data streams every 62 ms. The 32 byte payload is thus made up of 31 bytes of ECG data samples and 1 byte of RR data. This allows very close to real time processing and feedback of parameters for monitoring purposes.

G. Post-processing on Server

Once data is received on the remote server side, the data is reformatted and signal features are extracted to calculate HRV and RR. Based on test results the ECG data still contained 50 Hz AC interference, therefore, a digital notch filter was used to improve the final signal quality before feature extraction. This was easily implemented and and worked well in suppressing the remaining 50 Hz interference.

V. Results

A. Frequency Response of the Analog Frontend

Based on the hardware tests that were performed for analysis of hardware functionality, a frequency sweep was performed

to evaluate the response of the designed system. Here the simulated model's response was compared to that of the actual implemented hardware. The frequency sweep was performed between 0.1 Hz - 1 kHz for the simulation and between 0.1-250 Hz for the actual circuit. Figure 12 shows the simulated and measured frequency response for both the ECG and RR outputs.

Based on this response the actual implementation performed relatively well in isolating the required bandwidth. The only short coming from a hardware perspective was in filtering out the 50 Hz interference, the hardware implemented notch filter did not perform as well as expected. The implemented design also showed a much higher amplification of the signal, this could be as a result of the signal measured by the electrode having a higher impedance than anticipated in the simulations.

B. Raw Hardware Acquired vs. Final ECG Signal

Figure 13 shows a time based measurement of the ECG signal, here the raw hardware conditioned signal is compared to the digitally notch filtered signal. It is apparent that the implemented notch filter was not able to suppress all the AC interference as explained previously, this could be due to the fact that it is of a lower order. However, given the low frequency of interest and small bandwidth, for better noise suppression a much higher order filter would be required. This would increase the complexity of the hardware design and it was thus decided to implement further AC noise suppression in software on the server side. This allowed for the limitation of

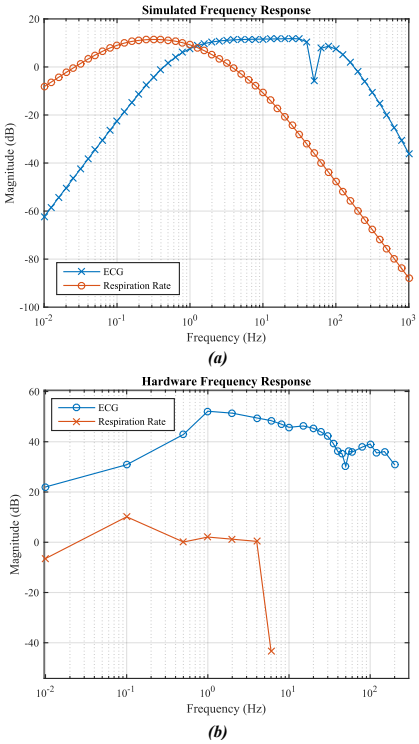

Fig. 12. (a) Shows the simulated frequency response of the system, while (b) shows the measured frequency response.

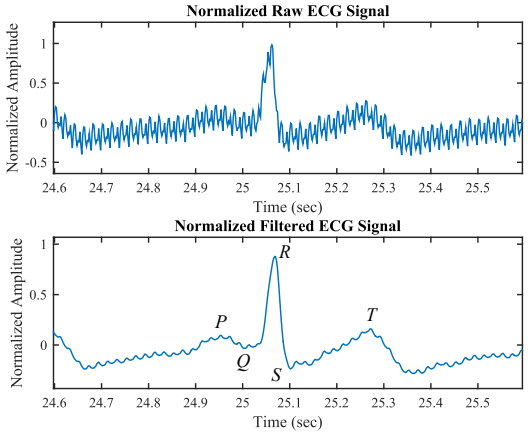

Fig. 13. Hardware acquired (raw) vs. filtered ECG signal response.

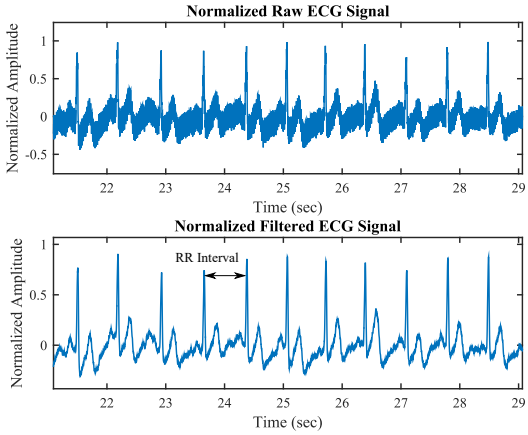

Fig. 14. A longer time frame of the raw vs. filtered ECG signal, notating the R-R interval.

hardware complexity at a very small cost in software processing. Once the excess AC interference has been removed the distinct features of the ECG signal clear and easily identifiable.

C. ECG Signal Evaluation

Evaluating the signal with regard to the discussed common ECG artifacts, the system was capable of suppressing any baseline wander. In figure 14 the raw and filtered ECG signals are compared over a longer time period to show how well the hardware performed. The R peaks are easily identifiable and extractable in software which are used for the purpose of calculating the R-R intervals, this can then be used to derive HRV.

D. Non-contact vs. Dry Contact

Based on the measurements obtained, it is apparent that the designed system can be implemented in both non-contact and dry contact configurations. Both signals are clear and features can be extracted after being digitally notch filtered. From figure 15 it is observed that the non-contact capacitively coupled approach does result in a slightly more distorted ECCG signal.

This is due to the enhanced sensitivity of the approach and is caused by small movements of the electrodes during breathing. The non-contact approach was placed on a thin cotton vest surface.

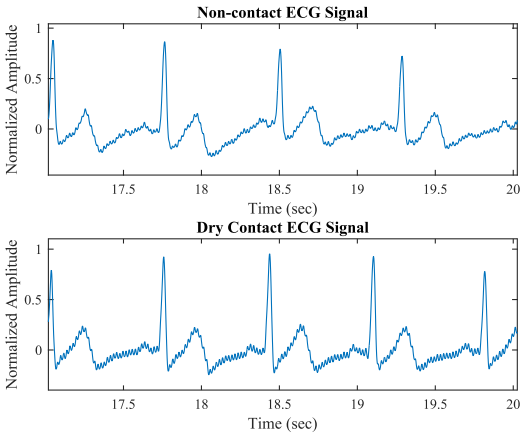

Fig. 15. Non-contact vs. dry contact ECG measurements.

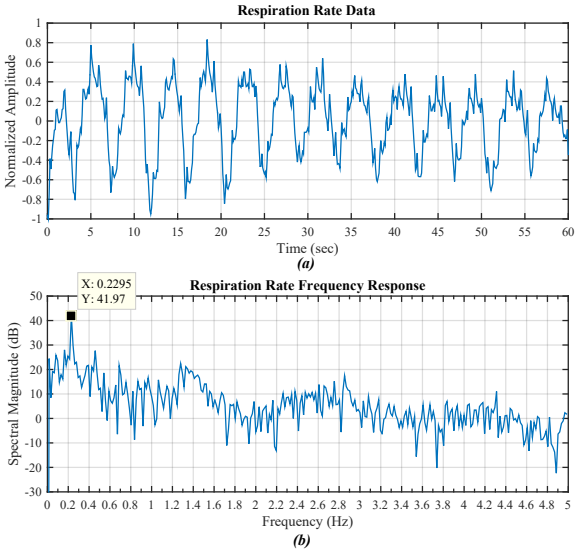

Fig. 16. (a) A time-based measure of the measured respiration rate signal, and (b) The frequency response of the measured respiration rate signal.

E. Respiration Rate

As for the sampled respiration rate signal, a clear low frequency signal component can be seen. The measured RR signal is given in figure 16 (a). The frequency domain of the RR signal was analysed to extract the key frequency component, which will indicate the actual measured respiration rate. Based on the results obtained this was achieved fairly accurately and in figure 16 (b) a dominant frequency of 0.2295 Hz is measured over a 60 second interval. From this the RR can be calculated as

$$\begin{aligned} RR &= f_{RR} \times 60 \\ &= 13.77 \\ &\approx 14BPM \end{aligned} \tag{7}$$

During the experimental measurement, the number of breathes taken was noted and corresponded to the measured result of 14 breathes in the 1 minute interval; thus showing sufficient accuracy.

F. System Hardware

The analog frontend and active electrodes were all designed with great care, keeping user safety and specifications in mind. The control unit was implemented on a breadboard level to test the design concepts, and the active electrode made use of non-surface mount technology. Figure 17 shows a graphical representation of the actual designed hardware solution.

VI. Future Work

The system performed well under the experimental test circumstances, and was evaluated under normal resting conditions and normal human movement. In order to ensure that the design works under all conditions it should be designed so that the system is integrated into a smart vest. This will ensure accurate continuous monitoring under any circumstances.

The system should also be optimised and minimised to a surface mount level on a PCB, this will allow for a more compact and mobile device, as well as easier integration with a smart vest. With regard to the 50 Hz AC interference which was not implemented with great success on a hardware level, it should be decided if it is worth it to increase hardware complexity or is a software implemented filter sufficient. The lack of AC suppression in hardware could also be due to the

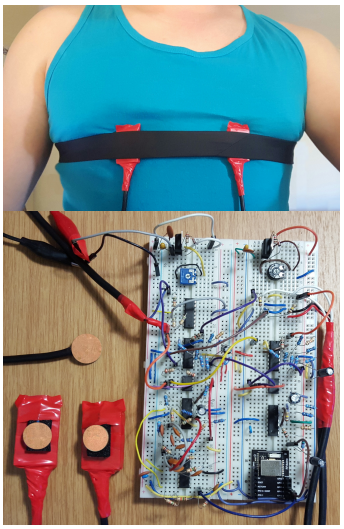

Fig. 17. Image of the active electrodes on the chest, and the final circuit implementation.

fact that the noise amplitude was much higher than that of the initial ECG signal, and that the implemented AC suppression was not enough.

VII. Conclusion

Taking the requirements for ubiquitous continuous health monitoring into consideration, the contactless or non-contact approach could be used for measuring ECG. It is also an important factor that the subject not be hindered or obstructed in any way, thus a minimalistic system with limited number of non-invasive sensors would be an excellent approach. The use of non-contact ECG to derive respiration rate is a promising solution that could potentially add value to this optimisation. The idea of implementing health monitoring devices into a smart vest has been done in some areas of research, and also proves as a promising prospect of future end user implementations.

In this work a wireless wearable system was designed capable of measuring ECG and respiration rate. The system makes use of the innovative approach of employing non-contact capacitive based active electrodes. Both ECG and respiration rate were measured using only the electrodes and an analog conditioning circuit. The device utilises BLE for low powered wireless communication to the remote server. The measured data could then be used to calculate HRV, RR and extract ECG related features. Based on the overall evaluation, the system's performance was deemed satisfactory and met the expectations of the proposed concepts. The obtained results were very closely related to that of the simulations and initial design concepts. Some future work is required to further develop the device into a promising prospect for continuous health monitoring.

References

[1] U. Varshney, "Pervasive Healthcare and Wireless Health Monitoring," *Mobile Networks and Applications*, vol. 12, no. 2-3, pp. 113–127, jul 2007.

[2] J. Wannenburg and R. Malekian, "Body Sensor Network for Mobile Health Monitoring, a Diagnosis and Anticipating System," *IEEE Sensors Journal*, vol. 15, no. 12, pp. 6839–6852, dec 2015.

[3] ——, "Physical activity recognition from smartphone accelerometer data for user context awareness sensing," *IEEE Transactions on Systems, Man and Cybernetics: Systems*, vol. 47, no. 12, pp. 3142–3149, dec 2017.

[4] P. Langley, E. J. Bowers, and A. Murray, "Principal component analysis as a tool for analyzing beat-to-beat changes in ECG features: application to ECG-derived respiration." *IEEE transactions on bio-medical engineering*, vol. 57, no. 4, pp. 821–9, apr 2010.

[5] A. C. Jose and R. Malekian, "Improving smart home security; integrating logical sensing into smart home," *IEEE Sensors Jounal*, vol. 17, no. 3, pp. 4269–4286, dec 2017.

[6] S. M. Lee, K. S. Sim, K. K. Kim, Y. G. Lim, and K. S. Park, "Thin and flexible active electrodes with shield for capacitive electrocardiogram measurement." *Medical & biological engineering & computing*, vol. 48, no. 5, pp. 447–57, may 2010.

[7] E. Nemati, M. Deen, and T. Mondal, "A wireless wearable ECG sensor for long-term applications," *IEEE Communications Magazine*, vol. 50, no. 1, pp. 36–43, jan 2012.

[8] J. S. Lee, J. Heo, W. K. Lee, Y. G. Lim, Y. H. Kim, and K. S. Park, "Flexible capacitive electrodes for minimizing motion artifacts in ambulatory electrocardiograms." *Sensors (Basel, Switzerland)*, vol. 14, no. 8, pp. 14 732–43, jan 2014.

[9] Gari D. Clifford, F. Azuaje, and P. McSharry, *Advanced Methods And Tools for ECG Data Analysis*, 1st ed. London: Artech house London, 2006.

[10] F. Gargiulo, A. Fratini, M. Sansone, and C. Sansone, "Subject identification via ECG fiducial-based systems: Influence of the type of QT interval correction," *Computer methods and programs in biomedicine*, vol. 121, no. 3, pp. 127–136, 2015.

[11] E. Sardini, M. Serpelloni, and M. Ometto, "Multi-parameters wireless shirt for physiological monitoring," in *2011 IEEE International Symposium on Medical Measurements and Applications*. IEEE, may 2011, pp. 316–321.

[12] Y. M. Chi, T.-P. Jung, and G. Cauwenberghs, "Dry-contact and non-contact biopotential electrodes: methodological review." *IEEE reviews in biomedical engineering*, vol. 3, pp. 106–19, jan 2010.

[13] J. W. Clark, M. R. Neuman, W. H. Olsen, R. A. Peura, F. P. Primiano, M. P. Siedband, J. G. Webster, and L. A. Wheeler, *Medical Instrumentation Application and Design*, 4th ed., J. G. Webster, Ed. John Wiley and Sons, Inc., 2009.

[14] H. Li and J. Tan, "Body sensor network based context aware QRS detection." *Conference proceedings : ... Annual International Conference of the IEEE Engineering in Medicine and Biology Society. IEEE Engineering in Medicine and Biology Society. Conference*, vol. 1, pp. 3266–3269, jan 2006.

[15] Y. M. Chi and G. Cauwenberghs, "Micropower non-contact EEG electrode with active common-mode noise suppression and input capacitance cancellation." *Annual International Conference of the IEEE Engineering in Medicine and Biology Society. IEEE Engineering in Medicine and Biology Society. Annual Conference*, vol. 2009, pp. 4218–21, jan 2009.

[16] D. K. Akinori Ueno, Tatsuya Imai and Y. Yama, *Biomedical Engineering*, C. A. B. de Mello, Ed. InTech, oct 2009.

[17] Y. M. Chi and G. Cauwenberghs, "Wireless Non-contact EEG/ECG Electrodes for Body Sensor Networks," in *2010 International Conference on Body Sensor Networks*. IEEE, jun 2010, pp. 297–301.

[18] Subhas C. Mukhopadhyay, *Wearable Electronics Sensors*, 1st ed., ser. Smart Sensors, Measurement and Instrumentation, S. C. Mukhopadhyay, Ed. Cham: Springer International Publishing, 2015, vol. 15.

[19] S. Coyle, K.-T. Lau, N. Moyna, D. O'Gorman, D. Diamond, F. Di Francesco, D. Costanzo, P. Salvo, M. G. Trivella, D. E. De Rossi, N. Taccini, R. Paradiso, J.-A. Porchet, A. Ridolfi, J. Luprano, C. Chuzel, T. Lanier, F. Revol-Cavalier, S. Schoumacker, V. Mourier, I. Chartier, R. Convert, H. De-Moncuit, and C. Bini, "BIOTEX–biosensing textiles for personalised healthcare management." *IEEE transactions on information technology in biomedicine : a publication of the IEEE Engineering in Medicine and Biology Society*, vol. 14, no. 2, pp. 364–70, mar 2010.

[20] Y. G. Lim, K. H. Hong, K. K. Kim, J. H. Shin, S. M. Lee, G. S. Chung, H. J. Baek, D.-U. Jeong, and K. S. Park, "Monitoring physiological signals using nonintrusive sensors installed in daily life equipment," *Biomedical Engineering Letters*, vol. 1, no. 1, pp. 11–20, mar 2011.

[21] G. Hahn, I. Sipinkova, F. Baisch, and G. Hellige, "Changes in the thoracic impedance distribution under different ventilatory conditions," *Physiological measurement*, vol. 16, no. 3A, p. A161, 1995.

[22] S. C. Mukhopadhyay, "Wearable Sensors for Human Activity Monitoring: A Review," *IEEE Sensors Journal*, vol. 15, no. 3, pp. 1321–1330, mar 2015.

[23] X. Zhu, W. Chen, T. Nemoto, Y. Kanemitsu, K.-i. Kitamura, K.-i. Yamakoshi, and D. Wei, "Real-time monitoring of respiration rhythm and pulse rate during sleep." *IEEE transactions on bio-medical engineering*, vol. 53, no. 12 Pt 1, pp. 2553–63, dec 2006.

[24] R. Pallás-Areny and J. G. Webster, *Analog signal processing*. John Wiley & Sons, 1999.